

# Aluminium adsorption on Ir(1 1 1) at a quarter monolayer coverage: A first-principles study

Hong Zhang<sup>a,b</sup>, Aloysius Soon<sup>b</sup>, Bernard Delley<sup>c</sup>, Catherine Stampfl<sup>b,\*</sup>

<sup>a</sup> School of Physical Science and Technology, Sichuan University, Chengdu 610065, PR China

<sup>b</sup> School of Physics, The University of Sydney, Sydney, New South Wales 2006, Australia

<sup>c</sup> Paul-Scherrer-Institut, CH-5232 Villigen PSI, Switzerland

Available online 9 February 2008

## Abstract

We present an *ab initio* density-functional study for aluminium adsorption on Ir(1 1 1) at high symmetry sites, namely, the fcc-, hcp-hollow, top and bridge sites. In each case, we calculate the atomic geometry, average binding energy, work function, and surface dipole moment at the coverage of 0.25 monolayer. We find the favourable structure to be Al at threefold hcp-hollow site, with a corresponding binding energy of 4.46 eV. We present and compare the electronic properties of the two lowest energy structures, i.e., at the threefold hollow sites and discuss the nature of the Al–Ir bond and binding site preference. In particular, we observe a large hybridization of Al-3s, 3p and Ir-5d states near Fermi level, forming an inter-metallic bonds. This results in a significant electron transfer from the Al atoms to the Ir(1 1 1) substrate, inducing an outward pointing surface dipole moment and a large decrease in the work function of 1.69 eV for Al in the hcp-hollow site. Compared to the fcc-hollow site, adsorption in the hcp-hollow site results in a lower density-of-states at the Fermi level, as well as a greater hybridization in the bonding states.

© 2008 Elsevier B.V. All rights reserved.

PACS : 81.65.Mq; 68.43. –h; 68.47.Gh

Keywords: Iridium; Binding energy; Aluminium adsorption; Work function; Density-functional theory

## 1. Introduction

Iridium-based alloys are important for developing ultrahigh-temperature oxidation-resistant coatings [1,2], due to their function as an effective oxygen diffusion barrier which is required for multilayered ultrahigh-temperature coatings. To avoid the formation of the toxic gaseous oxide, IrO<sub>3</sub>, iridium is usually alloyed with aluminium. It has been found that oxidized Ir/Al-based alloys can form protective double-layered coating structures, comprising of an iridium layer as an oxygen diffusion barrier followed by another layer of Al<sub>2</sub>O<sub>3</sub> layer to protect this barrier [3]. To understand the microscopic properties of such ultrahigh-temperature oxidation-resistant coatings, it is necessary to first understand the atomic and electronic structure of the Al/Ir alloy. In the present paper, we begin by studying the chemisorption of Al on Ir(1 1 1) using first-principles calculations. Experimentally, the interaction of

Al with an Ir(1 1 1) surface has been studied under ultra-high vacuum (UHV) conditions with Auger electron spectroscopy over a wide range of temperatures, i.e., from 300 to 2000 K [4]. At room temperature, layer-by-layer growth of an aluminium film was observed, which was commensurate with the substrate. However, at much higher temperatures (i.e., 1100–1300 K), a so-called “surface aluminide” is proposed to form and this phase decomposes at a temperature range of 1500–1900 K [4]. Detailed atomic and electronic structure of these low- and high-temperature phases are still lacking however, and to our knowledge, there are no further experimental or first-principles studies of this system. We consider adsorption of Al on Ir(1 1 1) at high symmetry sites, for a coverage of a quarter of a monolayer (ML) of Al. We first report the atomic geometry and binding energies, and proceed to analyze the electronic structure and bonding nature of Al–Ir.

## 2. Calculation method

All calculations are performed using density-functional theory (DFT) as implemented in the all-electron DMol<sup>3</sup> code

\* Corresponding author.

E-mail address: [stampfl@physics.usyd.edu.au](mailto:stampfl@physics.usyd.edu.au) (C. Stampfl).

[5,6], where we employ the generalized gradient approximation (GGA) of Perdew, Burke, Ernzerhof (PBE) [7] for the exchange-correlation functional. The Ir(1 1 1) surface is modeled using a supercell slab approach, where we use seven-layer Ir(1 1 1) slabs with a vacuum region of 25 Å. Aluminium atoms are adsorbed on both sides of the slab, preserving inversion symmetry. The aluminium atoms and the outmost two Ir layers are allowed to fully relax. The wave functions are expanded in terms of a double-numerical quality localized basis set with a real-space cutoff of 10 Bohr for both the bulk Ir and the surface. Polarization functions and scalar-relativistic corrections are also incorporated explicitly. The convergence criteria for the total energy, force on the atoms, and displacements are set to within  $1 \times 10^{-6}$  Ha ( $2.7 \times 10^{-5}$  eV),  $3 \times 10^{-4}$  Ha/Bohr ( $1.5 \times 10^{-2}$  eV/Å) and  $3 \times 10^{-4}$  Bohr ( $1.6 \times 10^{-2}$  Å), respectively. The Brillouin-zone integrations are performed using a  $(12 \times 12 \times 1)$  Monkhorst-Pack (MP) grid for the  $(1 \times 1)$  surface unit cell, yielding 19 special  $\mathbf{k}$ -points in the irreducible surface Brillouin-zone. The change in cohesive energy of bulk Ir is less than 10 meV per Ir atom when increasing the real space cutoff radius from 8 to 12 Bohr. The variation of the change in cohesive energy of bulk Ir is less than 3 meV per Ir atom when changing the  $\mathbf{k}$ -mesh from  $(6 \times 6 \times 6)$  to  $(16 \times 16 \times 16)$ . We thus adopt a cutoff radius of 10 Bohr and a MP  $\mathbf{k}$ -point mesh of  $(12 \times 12 \times 12)$ . For the surface calculations, we use the same cutoff radius with a MP  $\mathbf{k}$ -point mesh of  $(12 \times 12 \times 1)$  for the surface unit cell [8].

We address the stability of Al/Ir(1 1 1) structures with respect to adsorption of Al by calculating the average binding energy per Al adatom. The average binding energy per Al atom,  $E_b^{\text{Al/Ir}}$ , is defined as [9]:

$$E_b^{\text{Al/Ir}} = -\frac{1}{N_{\text{Al}}} [E^{\text{Al/Ir}} - (E^{\text{Ir}} + N_{\text{Al}}E^{\text{Al}})], \quad (1)$$

where  $N_{\text{Al}}$ ,  $E^{\text{Al/Ir}}$ ,  $E^{\text{Ir}}$  and  $E^{\text{Al}}$  are the number of Al atoms in the surface unit cell, the total energies of the adsorbate–substrate system, the clean surface, and the free Al atom, respectively. A spin-unrestricted calculation using non-spherical densities is performed for the aluminium atom. To achieve excellent numerical accuracy, the real-space cutoff for the calculation of the aluminium atom is increased to 20 Bohr, with the largest basis set available in the DMol<sup>3</sup> code. The binding energy is thus energy that a free Al atom gains upon adsorption on the Ir surface. A positive number indicates that the binding energy is exothermic with respect to the free Al atom, and a negative value endothermic.

To analyze the nature of bonding, we consider the difference electron density,  $n^{\Delta}(\mathbf{r})$ , which is defined as [9]:

$$n^{\Delta}(\mathbf{r}) = n^{\text{Al/Ir}}(\mathbf{r}) - n^{\text{Ir}}(\mathbf{r}) - n^{\text{Al}}(\mathbf{r}), \quad (2)$$

where  $n^{\text{Al/Ir}}(\mathbf{r})$ ,  $n^{\text{Al}}(\mathbf{r})$  and  $n^{\text{Ir}}(\mathbf{r})$  are the total electron densities of the adsorbate system, the clean surface, and that of the corresponding isolated Al adlayer. The atomic positions of the clean Ir surface and Al adlayers are taken to be the ones of the relaxed adsorbate system.

Using the Helmholtz equation, the surface dipole moment  $\mu$  (in Debye) is calculated according to the formula [10,11]:

$$\mu = \frac{A \Delta\Phi}{12\pi\Theta}, \quad (3)$$

where  $A$  is the surface area in Å<sup>2</sup> per  $(1 \times 1)$  surface unit cell,  $\Delta\Phi$  is the work-function change in eV, and  $\Theta$  is the coverage in ML.  $\Delta\Phi$  is calculated by taking the difference between the workfunction,  $\Phi$  of the adsorbate system and the clean surface, with  $\Phi$  being defined as the difference between the averaged electrostatic potential in the middle of the vacuum and the Fermi energy of the slab.

### 3. Results and discussions

The calculated bulk lattice constant of Ir is  $a_0 = 3.85$  Å, neglecting zero-point vibrations. The cohesive energy,  $E_{\text{coh}}$ , is calculated to be 7.45 eV and the bulk modulus,  $B = 3.57$  Mbar [8]. The corresponding experimental values are  $a_0 = 3.84$  Å,  $E_{\text{coh}} = 6.94$  eV, and  $B = 3.55$  Mbar [12]. The obtained interlayer relaxations of the clean Ir(1 1 1) surface,  $\Delta_{ij} = (d_{ij} - d)/d \times 100\%$ , between layers  $i$  and  $j$  with respect to the bulk spacing,  $d = 2.224$  Å, are  $\Delta_{12} = -1.57\%$  and  $\Delta_{23} = -0.49\%$  for the topmost layers. Early low energy electron diffraction experiments reported a contraction of the top Ir layer by 2.16 % [13].

We consider adsorption at the fcc- and hcp-hollow sites, the top site, and the bridge site. The binding energies  $E_b^{\text{Al/Ir}}$  of Al on the Ir(1 1 1) surface at these sites, at coverage 0.25 ML are listed in Table 1, given with respect to the free Al atom.

It can be seen from Table 1 that the hcp-hollow site is energetically favourable with a binding energy 4.46 eV at 0.25 ML, which is higher than the cohesive energy of Al bulk, with a value of 3.39 eV (experimental) [12] and 3.54 and 3.60 eV from DFT-GGA-PBE calculations using the pseudopotential and full-potential linearized–augmented plane-wave methods, respectively [14]. For the fcc hollow site, the binding energy is found to be very similar to that of hcp site, just 0.05 eV less favourable. The slightly more favourable adsorption energy of Al at the hcp-hollow site is also reflected by the slightly shorter Al–Ir bond length (2.47 Å compared to 2.49 Å). In order to check the effect of relaxation of interatomic layers deeper in the substrate, we perform a geometry relaxation with the outermost

Table 1

Calculated binding energy (in eV) and structural parameters (in Å) for an aluminium coverage of 0.25 ML at the fcc-, hcp-hollow, top and bridge sites

Adsorption site	Fcc-hollow	Hcp-hollow	Bridge	Top
Binding energy ( $E_b$ )	4.41	<b>4.46</b>	4.18	3.57
Bond-length ( $d_{\text{Al-Ir}}$ )	2.49	<b>2.47</b>	2.42	2.36
Vertical height ( $d_{01}$ )	1.91	<b>1.88</b>	1.96	2.35
Interlayer distance ( $\Delta_{12}$ )	-0.39	<b>-0.64</b>	-0.44	-0.89
Interlayer distance ( $\Delta_{23}$ )	-0.24	<b>-0.16</b>	-0.47	-0.31

$d_{\text{Al-Ir}}$  is the bond length between aluminium and the nearest surface iridium atom and  $d_{01}$  is the planar averaged vertical height of Al above the topmost Ir layer.  $\Delta_{12}$  and  $\Delta_{23}$  (in %) are the change in the first and second metal interlayer distances (with respect to the computed bulk spacing,  $d = 2.22$  Å) where the center of mass of the layer is used.

Table 2

Mulliken charge populations (in electrons) of the Al adatom and the corresponding (Al-bonded) surface Ir atom for the fcc-, hcp-hollow and top sites

	Al-3s	Al-3p	Ir-6s	Ir-6p	Ir-5d	Charge
Al at fcc-site ( $Al_{fcc}$ )	1.27	0.84	–	–	–	0.77
Surface Ir bonded to $Al_{fcc}$	–	–	0.96	0.73	7.60	–0.29
Al at hcp-site ( $Al_{hcp}$ )	1.26	0.86	–	–	–	0.75
Surface Ir bonded to $Al_{hcp}$	–	–	0.95	0.74	7.61	–0.30
Al at top-site ( $Al_{top}$ )	1.61	0.74	–	–	–	0.85
Surface Ir bonded to $Al_{top}$	–	–	0.99	0.65	7.50	–0.50

The aluminium coverage is 0.25 ML.

three Ir layers (as opposed to just two Ir layers) and Al adatom fully relaxed, for both the fcc- and hcp-hollow site. Indeed, we find an almost negligible effect on the binding energy ( $\sim 3$  meV). Thus the slight favouring of the hcp-site over the fcc-site is mainly due to effects from the first and second interatomic layers, i.e., due to the presence of an Ir atom in the second layer directly below the Al atom for the hcp-hollow site, while for the fcc-hollow site, there is no Ir atom directly below it in the second layer.

At this coverage of 0.25 ML, the binding energy of Al at the bridge site is 0.28 eV less favourable than that at the hcp-hollow site. This gives an estimate of the diffusion energy barrier of 0.28 eV, which is considerably lower than that for O on Ir(1 1 1) (0.65 eV) [8]. This is, in part, due to the stronger binding of O (4.62 eV) on Ir(1 1 1) than Al (4.46 eV). Once again, this is also captured in the notably shorter O–Ir bond length of 2.06 Å [8] as opposed to 2.47 Å in the Al–Ir bond.

With regard to the value of the calculated adsorption energy, Gall et al. [4] reported an estimated activation energy,  $E_{des}$ , for thermal desorption of Al atoms from the (1 1 1) surface of iridium from thermal desorption data of about 3.5–4.5 eV, assuming that all surface atoms have an equal probability of desorbing, and that the desorption flux from the surface obeys the Arrhenius relation. The value of  $E_{des}$  is thus consistent with our calculated binding energy. We now consider the electronic structure of the Al/Ir(1 1 1) system. The electron charge population for Al on Ir(1 1 1) at the fcc-, hcp-hollow and top sites are listed out in Table 2. The charge populations are calculated by the Mulliken charge population analysis. Due to the limitations of this type of analysis [15], the charges can only be considered in qualitative terms. It can be seen that there is a charge transfer from the Al atoms to the nearest neighboring Ir atoms. For Al in the favoured hcp-hollow site, the value is about 0.75 e. A similar value of 0.77 e is seen for Al at the fcc-hollow site. In contrast, the charge transfer is about 0.85 e when Al is at the top site. This indicates that the electron redistribution is rather similar for Al at each of the threefold hollow sites.

This partial charge transfer is also reflected in the difference electron density distribution shown in Fig. 1, where electron transfer from the Al atom towards the 6s and 6p states of the nearest-neighbour Ir atoms can be clearly seen. There is also a polarization of the surface Ir atoms. This is similar to the behaviour reported for Pt/Al(1 1 1) system [16]. The formation of an Al–Ir bond induces a rather similar redistribution of charge for the fcc-hollow site and the hcp-hollow site. This redistribution induces an outward pointing

surface dipole moment, giving rise to a decrease in the work function of the clean surface of 1.69 eV for Al at the favoured hcp-hollow site. The calculated surface dipole moment,  $\mu$ , is  $-1.15$  Debye according to Eq. 3. The work function for clean Ir(1 1 1) and Al/Ir(1 1 1) at the hcp-hollow site is calculated to be 5.88 and 4.19 eV, respectively.

To provide further insight into the electronic structure of this system, we consider the projected density-of-states (PDOS) of both threefold hollow sites, as shown in Fig. 2 (a) and (b). In both cases, we see a strong overlap of Al-3s and Ir-5d states at around about 5.2 eV below the Fermi level, and an effective (bonding) hybridization between Ir-6s and 5d states at around 6.5 eV below the Fermi level. However, there are a few notable differences: The Ir-5d states for Al adsorption at the hcp-hollow site (see Fig. 2(b)) is slightly broader than that at the fcc-hollow site (see Fig. 2(a)), suggesting a greater hybridization of states for Al at the hcp-hollow site (e.g., of Ir-6s and 5d and of the Al-3s and Ir-5d). In addition, at the Fermi level, the Ir-5d states are higher for Al at the fcc-hollow site compared to that at the hcp-hollow site, which indicates that Al adsorption at the fcc-hollow site is less stable. These differences in the PDOS, thus suggest why Al could be expected to adsorb slightly more favourably at the hcp-hollow site.

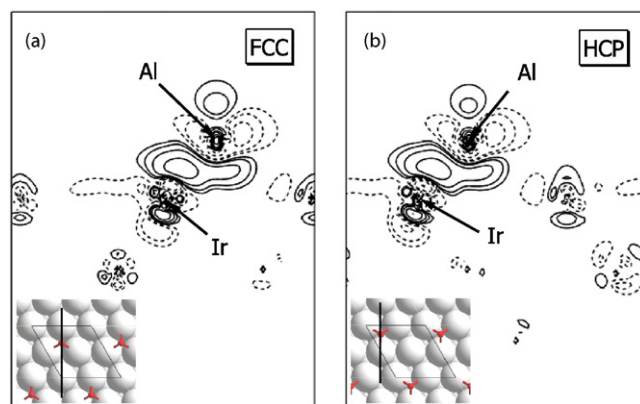


Fig. 1. (Colour online) Difference electron density plot for 0.25 ML of aluminium adsorbed on Ir(1 1 1) at (a) the fcc-hollow and (b) the hcp-hollow site. Inserts show the top-view of the atomic structure of Al/Ir(1 1 1) at the fcc-hollow and hcp-hollow site, respectively. Ir substrate atoms are represented by large spheres while Al adatoms are shown as small circles. For each site, a dot-dashed line is drawn to show the plane in which the difference electron density contour plot is drawn. For the contour plots, dashed lines represent charge depletion and solid lines charge accumulation. The lowest positive contour line is at  $0.001 \text{ e Bohr}^{-3}$  while the highest negative contour line corresponds to a value of  $-0.001 \text{ e Bohr}^{-3}$ . In between, the electron density changes successively by a factor of  $10^{1/3} \text{ e Bohr}^{-3}$ .

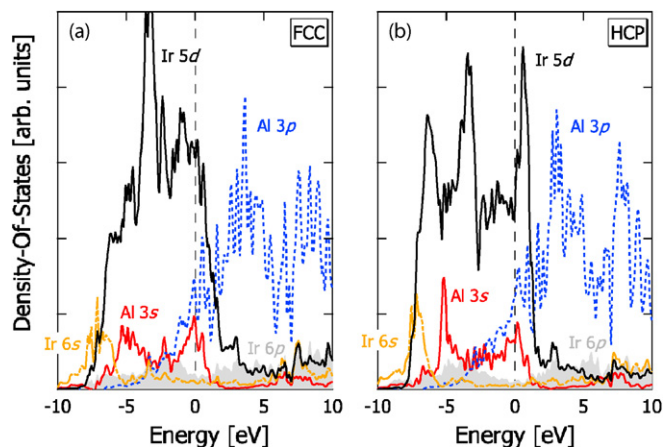


Fig. 2. (Colour online) Projected density-of-states for 0.25 ML of aluminium adsorbed on Ir(1 1 1) at (a) the fcc-hollow and (b) the hcp-hollow site. The dark (black) continuous line represents the 5d states of the Ir atom bonded to the Al adatom. Ir-6s states are plotted in the light (orange) dot-dashed line, and 6p states are shaded in light grey. Al-3s states are shown as a dark (red) continuous line, while the 3p states are plotted in a dark (blue) dotted line. The Fermi level is indicated by the vertical dashed line at 0 eV.

Thus by inspecting both the atomic and electronic structure of Al/Ir(1 1 1), we find that the slight favouring of Al adsorbing at the hcp-hollow site over the fcc-hollow site arises from the broader Ir-5d states and more effective overlap of the bonding states and a reduced DOS at the Fermi level, coupled with (and inducing) a slight shortening of the Al–Ir bondlength.

#### 4. Conclusion

For the coverage of a quarter monolayer, the physical and electronic properties associated with Al adsorption on Ir(1 1 1) at the fcc, hcp, top and bridge sites were investigated using first-principles DFT-GGA calculations. We find that Al adsorption at the hcp-hollow site is energetically most favourable, with a binding energy of 4.46 eV. There is a significant electron transfer from Al atom to the Ir(1 1 1) substrate, inducing an outward pointing surface dipole moment, resulting in a large decrease in the work function of 1.69 eV. We find that the Al–Ir bondlength is slightly shorter for Al at the hcp-hollow site and

this supports the slightly favourable hcp-hollow site. The projected density-of-states (PDOS) also shows that there is a significant hybridization of Al-3s, 3p and Ir-5d states near Fermi level, forming inter-metallic bonds. The slight preference of Al adsorption at the hcp-hollow site is reflected in the greater broadening of the Ir-5d states which affords more effective hybridization of states, as well as a lower DOS at the Fermi level which promotes the stability of Al at the hcp-hollow site.

#### Acknowledgments

The authors gratefully acknowledge support from the Australian Research Council (ARC), the Australian Partnership for Advanced Computing (APAC) and the Australian Centre for Advanced Computing and Communications (ac3).

#### References

- [1] K.N. Lee, W.L. Worrell, *Oxid. Met.* 32 (1989) 357–369.
- [2] K.N. Lee, W.L. Worrell, *Oxid. Met.* 41 (1994) 37–63.
- [3] H. Hosoda, S. Miyazaki, S. Hanada, *Intermetallics* 8 (2000) 1081–1090.
- [4] N.R. Gall, E.V. Rut'kov, A.Ya. Tontegode, *Phys. Solid State.* 48 (2006) 369–376.
- [5] B. Delley, *J. Chem. Phys.* 92 (1990) 508–517.
- [6] B. Delley, *J. Chem. Phys.* 113 (2000) 7756–7764.
- [7] J.P. Perdew, K. Burke, M. Ernzerhof, *Phys. Rev. Lett.* 77 (1996) 3865–3868.
- [8] H. Zhang, A. Soon, B. Delley, C. Stampfl, in preparation.
- [9] M. Scheffler, C. Stampfl, *Theory of adsorption on metal substrates*, in: K. Horn, M. Scheffler (Eds.), *Handbook of Surface Science*, Vol. 2. Electronic Structure, Elsevier, Amsterdam, 2000, pp. 286–357.
- [10] L.D. Schmidt, R. Gomer, *J. Chem. Phys.* (1966) 1605–1623.
- [11] L.W. Wanson, R.W. Strayer, *J. Chem. Phys.* 48 (1968) 2421–2442.
- [12] C. Kittel, *Introduction to Solid State Physics*, John Wiley & Sons Inc., 1986.
- [13] C.M. Chan, S.L. Cunningham, M.A. Van Hove, W.H. Weinberg, S.P. Withrow, *Surf. Sci.* 66 (1977) 394–404.
- [14] M. Fuchs, J.L.F. Da Silva, C. Stampfl, J. Neugebauer, M. Scheffler, *Phys. Rev. B* 65 (245212) (2002) 1–13.
- [15] A. Szabo, N.S. Ostlund, *Modern Quantum Chemistry*, McGraw-Hill, New York, 1989.
- [16] J.A. Rodriguez, M. Kuhn, *Chem. Phys. Lett.* 240 (1995) 435–441.